CIRCULATION COPY
SUBJECT TO RECALL
IN TWO WEEKS

387-06

UCRL-88996

Graded-index surfaces and films

W. Howard Lowdermilk*

Lawrence Livermore National Laboratory, University of California
P.O. Box 5508, L-490, Livermore, California 94550

Abstract

Reducing or eliminating reflectance of electromagnetic radiation from surfaces has important technical and commercial applications. Graded-index surfaces are of interest because they have low reflectivity over much broader spectral regions and angles of incidence than conventional thin film coatings.

This paper reviews methods to calculate the reflectivity and to estimate the refractive-index profile of graded-index surfaces. Charactertistic properties and techniques to produce graded-index surfaces are reviewed. The results of recent measurements of laser-induced damage to graded-index surfaces are summarized.

Introduction

Graded-index surfaces and films are primarily of interest for their broadband, anti-reflective (AR) property. Because of this property, they have important applications in solar energy collecting systems,[1-7] where they are used to increase either transmission or absorption of the substrate material. Recently, graded-index AR surfaces also have been found to be more resistant to damage by intense laser beams than thin film AR coatings.[8-12] They are consequently finding important applications in high power laser systems. Other applications for graded-index surfaces include anti-glare display cases and optical disks whose surfaces are written upon by laser beams.

There are now a variety of techniques to produce graded-index surfaces and films. Their properties depend on the method by which they are produced. This paper is concerned only with non-absorbing graded-index surfaces and films for use with visible and near-infrared light to increase transmission through the substrate material. The principal method to produce such surfaces and films is by chemical leaching and etching. This process removes certain components of the surface and leaves or redeposits others in such manner as to create a porous, skeletonized surface layer. When the pore dimensions are much smaller than the wavelength of the incident light, little scattering occurs and the surface layer has effectively a low index of refraction.

The refractive index and porosity of the surface layer may be estimated using the Clausius-Mossotti relation. The refractive index n_g of a glass composed of ν ionic species is given by the expression

$$\frac{n_g^2-1}{n_g^2+2} = \frac{4}{3}\pi \sum_1^{\nu} \alpha_i N_i \,, \tag{1}$$

where α is the polarizability of the ionic oscillator and N is the number per unit volume. If the ionic polarizability remains unchanged by the leaching process, then the refractive index n_f of the surface layer is given by

$$\frac{n_f^2-1}{n_f^2+2} = \frac{4}{3}\pi \sum_2^{\nu} \alpha_i N_i \,. \tag{2}$$

The volume fraction of glass remaining after leaching is

$$V = \sum_2^{\nu} N_i / \sum_1^{\nu} N_i \,. \tag{3}$$

Using Equations 1 and 2, with the approximation that all ionic species have the same polarizability and volume gives

*Work performed under the auspices of the U.S. Dept. of Energy by Lawrence Livermore National Laboratory under contract No. W-7405-ENG-48.

DISCLAIMER

This document was prepared as an account of work sponsored by an agency of the United States Government. Neither the United States Government nor the University of California nor any of their employees, makes any warranty, express or implied, or assumes any legal liability or responsibility for the accuracy, completeness, or usefulness of any information, apparatus, product, or process disclosed, or represents that its use would not infringe privately owned rights. Reference herein to any specific commercial product, process, or service by trade name, trademark, manufacturer, or otherwise, does not necessarily constitute or imply its endorsement, recommendation, or favoring by the United States Government or the University of California. The views and opinions of authors expressed herein do not necessarily state or reflect those of the United States Government or the University of California, and shall not be used for advertising or product endorsement purposes.

This report has been reproduced
directly from the best available copy.

Available to DOE and DOE contractors from the
Office of Scientific and Technical Information
P.O. Box 62, Oak Ridge, TN 37831
Prices available from (615) 576-8401, FTS 626-8401

Available to the public from the
National Technical Information Service
U.S. Department of Commerce
5285 Port Royal Rd.,
Springfield, VA 22161

Work performed under the auspices of the U.S. Department of Energy by Lawrence Livermore National Laboratory under Contract W-7405-ENG-48.

BEST AVAILABLE COPY

FOR ORIGINAL REPORT

CALL

REPORTS LIBRARY

X37097

$$V = \frac{(n_f^2 - 1)(n_g^2 + 2)}{(n_f^2 + 2)(n_g^2 - 1)} \quad . \tag{4}$$

For values of n_g and n_f not much larger than 1, Equation 4 gives the following simple relation between refractive indices and volume fraction:

$$n_f = n_g V + (1-V) \quad . \tag{5}$$

Equation 5 assumes that the pores are filled with air and therefore have refractive index $n_p = 1$. If the pores begin to fill with some other substance, for example water from the atmosphere, the effective index of the pores becomes

$$n_p = n_w v_w + 1 - v_w \quad , \tag{6}$$

where v_w is the fraction of the pore volume filled with water, and n_w is the refractive index of the water. Equation 5 then becomes

$$n_f = n_g V + n_p (1-V) \quad . \tag{7}$$

Calculating the reflectance of graded-index surfaces

Graded-index surfaces are characterized by a strong, continuous variation in the refractive index in the direction of the normal to the surface. The region of graded-index may be bounded by discontinuities in the refractive index. Figure 1 shows an example of the refractive index profile which may be produced by the techniques discussed in later sections. It is assumed that the refractive index is constant over any plane parallel to the surface.

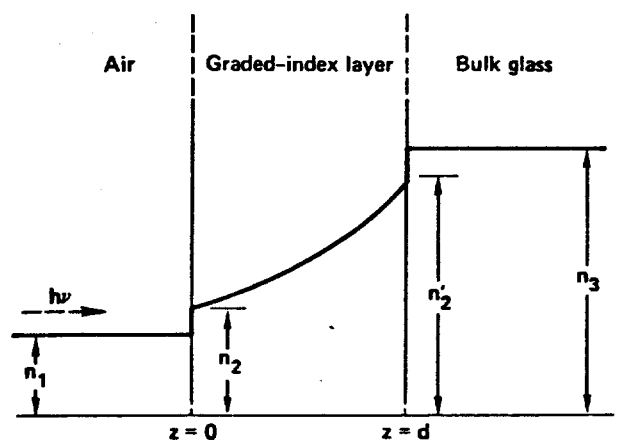

Figure 1: Refractive index profile of a typical graded-index surface layer.

A general theory of light reflection from graded-index surfaces is given by R. Jacobsson.[13] When the refractive index varies strongly, which is generally true of graded-index AR surfaces, the theoretical treatment is difficult because the wave equation can be solved explicitly in terms of known functions in only a few special cases. Even then the expressions are complicated and of limited value for direct numerical work. For example, an exponential profile[14,15] gives a reflectance in terms of Bessel functions of integral order, while a linear profile[15] gives Bessel functions of order one-third.

However, with the use of computers, extensive numerical calculations can easily be performed for profiles of any shape. Two different numerical approaches may be taken to calculate the reflected intensity. One method is to approximate the graded-index layer by a large number of very thin, homogeneous layers and calculate the reflectance by multiplication of the characteristic matrices representing the individual thin layers.[16] The second method is to numerically integrate the second-order wave equation.[17]

An example is shown in Figure 2 of a calculation made by the matrix method. The index profile of the graded-index layer used in this calculation is shown in the inset. The index varied from 1.0 to 1.5 with small discontinuities at the boundaries of the layer. This layer was divided into 100 thin layers to calculate the intensity reflected at normal

incidence versus the ratio of the thickness d of the graded layer to the wavelength λ of the incident light.

Other examples calculated by the matrix method are shown in Figure 3. This figure gives calculated reflectivities for various graded-index profiles between n = 1 and n = 1.6.

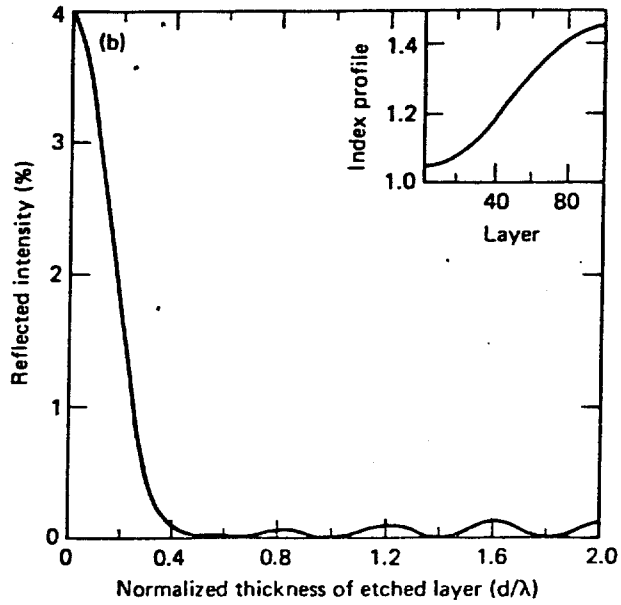

Figure 2: Reflectivity versus normalized depth of graded-index layer calculated for the refractive index profile shown in the inset.

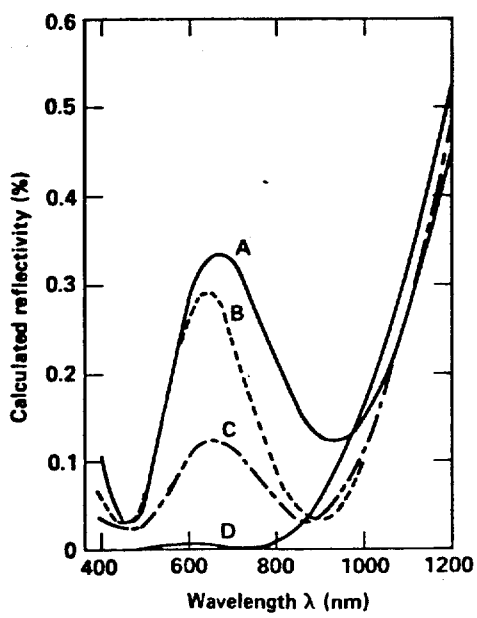

Figure 3: Calculated reflectivity for different graded-index transition layers between air (n_1=1) and a substrate with n_3=1.6: (a) n changes linearly with depth z; (b) n changes linearly with optical depth nz; (c) n changes quadratically with depth; and (d) the change of index is described by a Gaussian. From E. Spiller et al, Reference 67.

Curve A represents a linear increase in refractive index with the geometrical coordinate. For curve B, the refractive index increases linearily with the optical thickness of the layer. The refractive index variation for curve C was the quadratic function

$$n = 1 + 0.6\ (z/z_0)^2,$$

where the spatial coordinate $z = 0$ corresponds to the bottom of the transition layer, and the value $z = z_0 = 0.45\mu m$ corresponds to the air interface. For curve D, the index profile was the Gaussian function

$$n = 1 + 0.6 \exp - (z/z_0)^2,$$

with $z_0 = 0.25\mu m$.

Figure 4 gives additional examples. The calculations in this case were made by the direct integration method for light incident at 45° on various graded-index profiles between n = 1 and n = 1.5.

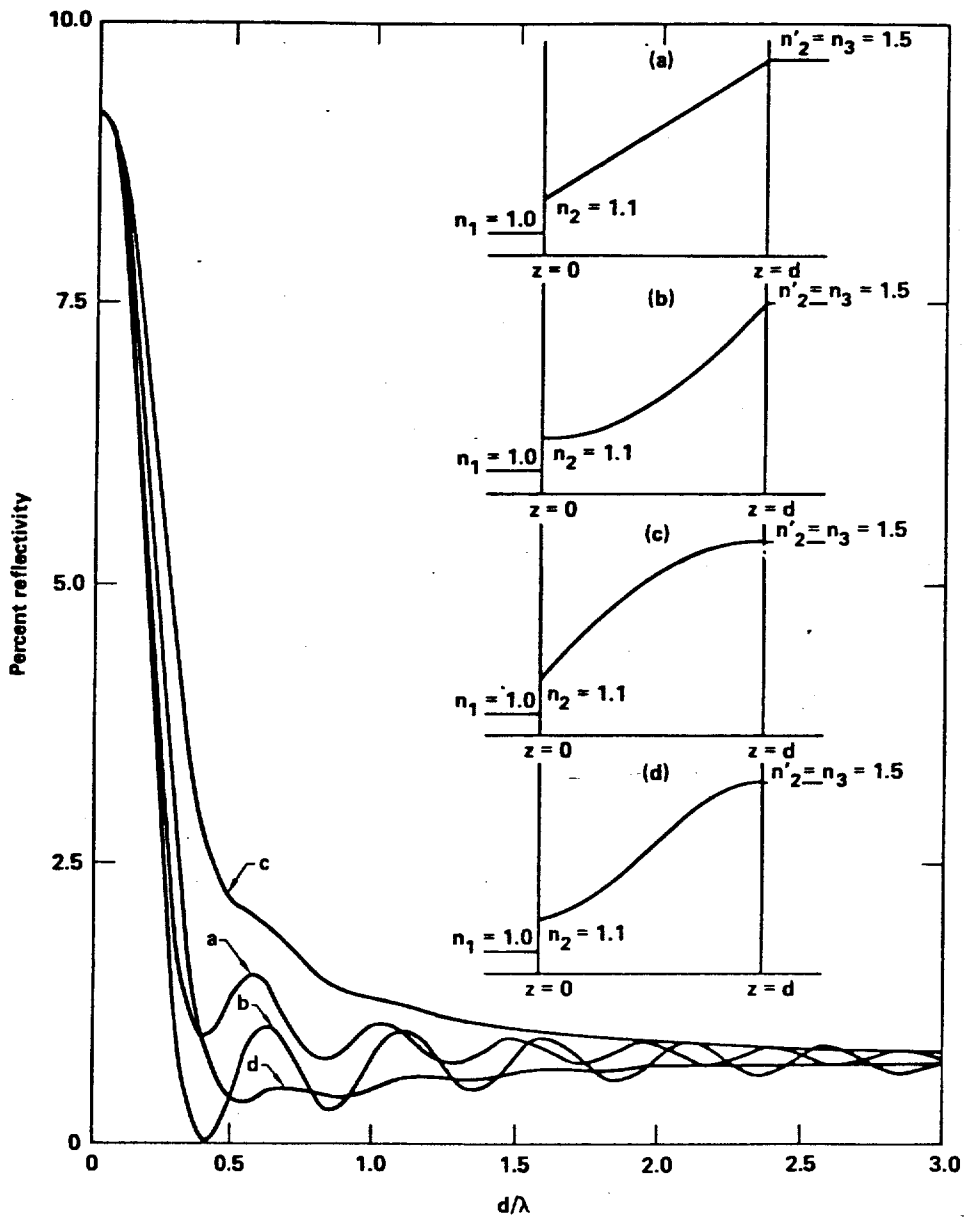

Figure 4: Reflectance of TE wave at 45° angle of incidence for (a) linear ramp profile, (b) concave parabolic profile, (c) convex parabolic profile, (d) cubic profile. From B. Sheldon et al, Reference 17.

Estimating the index profile from the measured reflectance spectrum

General Case

The oscillations in reflectance versus d/λ shown in Figures 2-4 are characteristic of the index profile. Sheldon et al[17] found that these oscillations have nearly a constant period. This period, when plotted versus angle of incidence, gives a curve which is sensitive to the shape of the refractive index profile. The index profile may then be deduced from the reflectance measurements by a simple graphical procedure.

Linear Ramp Profile

Often the index profile may be approximated reasonably well by a linear ramp (see Figure 4a). Reflectance from the linear ramp profile was analyzed by Schroeder.[18] The reflectivity at normal incidence is approximately

$$R \simeq 1 - \frac{4n_2n_2'n_3}{[n_2n_3+n_2']^2 - [n_2^2-1][n_3^2-n_2'^2]\sin^2\delta/2}, \tag{8}$$

where

$$\delta = \frac{2\pi}{\lambda}[n_2 + n_2']\,d \quad . \tag{9}$$

The minimum and maximum reflectivities are

$$R_{min} = \left[\frac{n_2n_2'-n_3}{n_2n_2'+n_3}\right]^2 \quad \text{at } \lambda = 2\,[n_2+n_2']\,d/(2m+1) \quad , \tag{10}$$

$$R_{max} = \left[\frac{n_2n_3-n_2'}{n_2n_3+n_2'}\right]^2 \quad \text{at } \lambda = 2\,[n_2+n_2']\,d/2m \quad , \tag{11}$$

for integer values of m.

Substituting measured values of R_{max} and R_{min} and the wavelengths at which they occur, along with the known value n_3, into Equations 10 and 11 allows calculation of n_2, n'_2 and d. Those values may then be used in Equation 8 to calculate the reflectance spectrum for the linear ramp. Comparison of the calculated and measured reflectance spectrum will determine whether the linear ramp profile was a reasonable approximation to the actual index profile.

Properties of graded-index surfaces

The most important properties of graded-index surfaces for applications are insensitivity of the intensity of reflected light to:

- Thickness of the graded-index layer
- Wavelength of the incident light
- Angle of incidence of light on the surface

For the index profile in Figure 2, for example, increasing the thickness of the graded-index layer while holding λ constant reduces the reflected intensity from 4% for d = 0 to zero for $d = 0.7\lambda$. As the thickness of the layer increases further, the reflectivity varies periodically, due in part to interference between the reflected components from the index discontinuities at the layer boundaries, but remains below 0.1%. In contrast, the reflectance of a discrete homogeneous layer varies as shown in Figure 5, with successive minima and maxima at intervals of quarterwave optical thickness of the film.

Figure 2 may also be used to illustrate that for a graded-index layer of fixed thickness, the surface is approximately antireflective for wavelengths $\lambda < 2.5d$.

Since the intensity reflected at normal incidence is insensitive to the optical thickness of the graded-index layer, one would expect the reflectance also to be insensitive to angle of incidence of the light on the surface. Calculations by Minot[19], summarized in Figure 6, show the reflectivity is approximately independent of incident angle for angles less than 50°. Reflectivity is also significantly reduced for even larger angles of incidence.

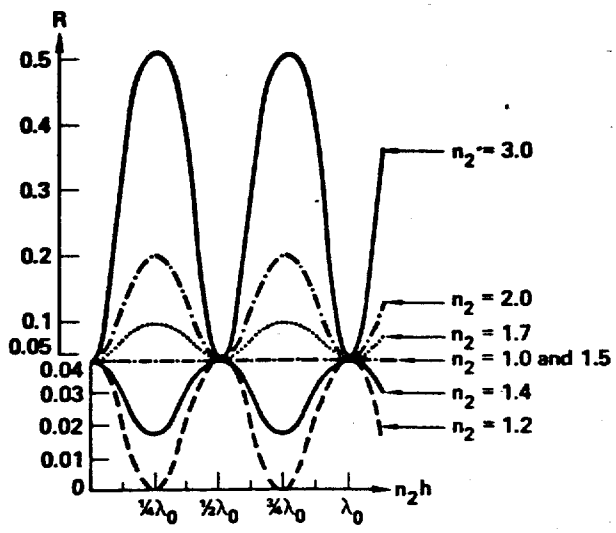

Figure 5: Reflectivity at normal incidence of a dielectric film of refractive index n_2 as a function of its optical thickness (n_1=1, n_3=1.5). From M. Born and E. Wolf, Principles of Optics, Pergamon Press, London, 1470, p. 64.

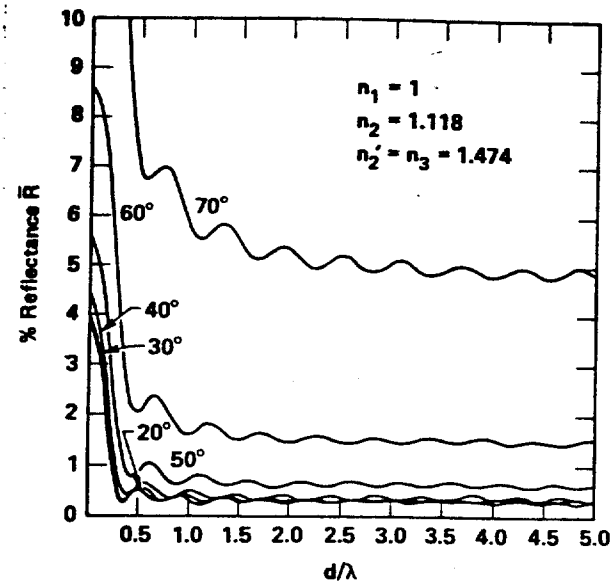

Figure 6: Computer-calculated average reflectance $R=1/2(R_s+R_p)$ as a function of angle of incidence, plotted against d/λ for graded-index layer with linear ramp profile where n_1=1, n_2=1.118, n_2=n_3=1.474. From M. J. Minot, Reference 19.

Techniques to produce graded-index surfaces

The techniques for producing graded-index AR surfaces have in common a leaching or etching step which creates a surface layer with microscopic porosity. The formation of antireflective surfaces on glass by chemical etching was known long before thin film coatings were developed for that purpose. Fraunhofer[20] and Rayleigh[21] noted the reduction in reflectivity of glass tarnished by exposure to acid. A more complete history of this early work is given by Cook and Mader.[22] The technology to produce AR surfaces by chemical etching was introduced by Taylor[23], Kollmorgen[24] and Amy.[25] However, it was not until the late 1930's that acid treatments to reduce surface reflectivity came into popular use.[26] The first technique used commercially was the RCA "Magicote C" process.[27-33] However, practical applications of AR films produced by chemical etching generally were limited because the surfaces were difficult to develop reproducibly, were optically inefficient and lacked physical durability.[34] In addition, rapid advance in the technology of vacuum-evaporation led soon to replacement of chemical etching by multilayer, thin-film AR coatings.

In recent years, the interest in chemical leaching techniques has been renewed, primarily by requirements for very inexpensive, broadband AR coatings for solar receptors. For example, the use of glass with an AR surface for cover plates on flat plate solar-thermal collectors permits the extractable heat to be increased by 30-50% compared with their performance without broadband AR coatings under equivalent solar flux, surface temperature and ambient conditions.[6] Chemically etched AR surfaces were also found to have laser damage thresholds more than two times greater than thin-film AR coatings. This discovery prompted development of glasses and etching methods to produce AR surfaces on glass of high optical quality.

Phase-Separated Glass

Minot[35-37] produced graded-index AR surfaces by etching phase-separated glass. Phase separation in alkali borosilicates is well known.[38,39] Under appropriate heat treatment, these glasses separate into a relatively insoluble, silica-rich phase and a more soluble phase consisting primarily of B_2O_3 and Na_2O.[40] The soluble phase can be preferentially leached away leaving an interconnected network of pores and solid glass consisting primarily of the silica-rich phase. The volume fraction of remaining glass decreases through the film toward the surface.

The size of the pores, typically 10-100 Å diameter, can be controlled by the original glass composition, the heat treatment and the etch/leach process. Minot optimized the process empirically with respect to optical properties for AR surfaces on Corning Code 7740 glass (Pyrex™). Further studies on processing Code 7740 glass were made by Elmer and Martin.[41] Approximate characterisitcs of the optimized process are as follows:

Glass composition - Code 7740 (in wt%)
SiO_2-81%, B_2O_3-13%, Al_2O_3-2%, Na_2O-4%

Etching chemicals
Reagent grade nitric acid, ammonium fluoride and hydrofluoric acid.
Technical grade ammonium bifluoride.
Distilled water.

Heat Treatment
Glass specimens heated in an electric furnace for 3 hrs at temperatures of 600-680°C.
Solutions heated in plastic containers in a hot water bath.

Surface Treatment
Pre etch in 10 wt% ammonium bifluoride solution at room temperature for 20 min.
Rinse in distilled water for 30 seconds.
Selective etch in desired solution, generally at 90°C for 5 min.
Soak in distilled water at room temperature for 2 min.
Dip in alcohol and dry at room temperature.

Reflectance and transmission versus wavelength
The reflectance and transmittance of treated and untreated samples for wavelengths in the visible and near infrared are shown in Figure 7. The samples were heat treated at 630°C and etched in 1N HNO_3 containing NH_4HF_2.

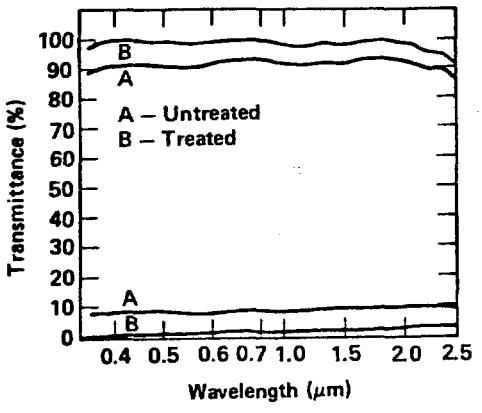

Figure 7: Reflectance(lower curves) and transmittance (upper curves) of treated and untreated samples vs. wavelength in visible and near infrared. From T. H. Elmer and F. W. Martin, Reference 41.

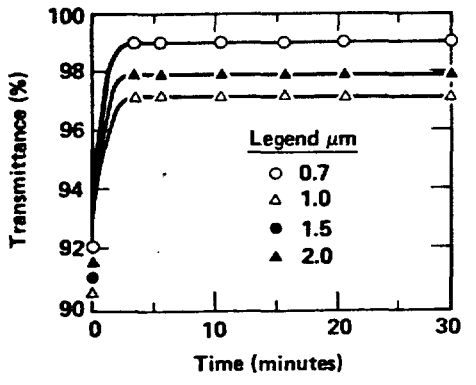

Figure 8: Transmittance of Code 7740 glass as a function of time of treatment in 0.3 wt% $NH_4F \cdot HF$ dissolved in 1N HNO_3 heat treatment for 3 h at 630°C followed by cooling at 100°C/h.

Transmittance versus time in the solution for glass heat-treated at 630°C for 3 hrs
Solution: 1N HNO_3 + 0.4 wt% $NH_4F \cdot HF$ at 90°C
Wavelength range 0.4-0.7μm
Transmittance for wavelengths of 0.4-0.7μm are given in Table 1.
Wavelength range 0.7-2.0μm
Transmittance for wavelengths of 0.7-2.0μm are given in Figure 8.
Solution: 0.16 N HNO_3 + 0.6 wt% NH_4F at 90°C
Wavelength range 0.4-0.7μm
Transmittance for wavelengths of 0.4-0.7μm are given in Table 2.
Wavelength range 0.7-2.0μm
Transmittance for wavelengths of 0.7-2.0μm are given in Figure 9.

Durability
Power and Elmer[42] reported that the solar transmittance of treated Code 7740 glass remained virtually unchanged after 37 months continuous exposure to weather.

Table 1. Transmittance of 630°C Heat-Treated Code 7740 Glass Treated in 1N HNO_3 + 0.4 wt% $NH_4F \cdot HF$ at 90°C. From T. H. Elmer and F. W. Martin, Reference 41.

Treatment time (min)	Transmittance at 0.4-0.7μm			
	0.4	0.5	0.6	0.7
0	91.6	91.7	91.9	92.0
3	99.0	99.0	99.0	98.8
5	99.4	99.6	99.0	98.8
10	99.4	99.6	99.3	99.0
15	99.5	99.3	98.9	99.1
20	99.6	99.6	98.8	99.0
30	99.6	99.6	98.8	99.5

Table 2. Transmittance of 630°C Heat-Treated Code 7740 Glass Treated in 0.16N HNO_3 + 0.6 wt% NH_4F at 90°C. From T. H. Elmer and F. W. Martin, Reference 41.

Treatment time (min)	Transmittance at 0.4-0.7μm			
	0.4	0.5	0.6	0.7
0	92.1	92.0	92.1	92.1
0.5	98.9	89.9	98.2	97.4
1	99.0	99.0	98.5	98.0
2	99.0	99.0	98.5	98.3
4	99.8	99.8	99.0	98.5
6	99.8	99.8	99.0	98.7
10	99.0	99.4	99.0	98.0
15	99.4	99.5	99.0	98.0
20	99.6	99.5	99.0	98.0
30	99.8	99.5	99.0	98.0

Phase-Separated, Optical Quality Glass

Graded-index AR surfaces on Corning Code 7740 glass exhibited much higher thresholds for damage by pulsed Nd-glass lasers than thin-film AR coatings.[8,9] As a result, the possibility of graded-index surfaces for high power laser applications became of interest. However, Corning Code 7740 glass has a high silica content and high melting temperature, which make it difficult to produce with optical quality. To meet this need, Hoya developed an optical quality, phase separable glass, ARG 2. Its properties and graded-index surface formation were reported by Asahara and Izumitani.[43]

Properties of ARG 2 glass. The properties of ARG 2 are given and compared with other optical glass in Table 3.

Antireflection treatment. Samples were heat treated at 570°C for 3 hrs, then leached in an aqueous solution of 0.1% $NH_4F \cdot HF$ and 1.0% HNO_3 for 10 min at 75°C.

Reflectance and transmittance versus wavelength. Reflectance and transmittance for ARG 2 glass after heat treatment and leaching is shown in Figure 10.

Dependence of reflectivity on leaching time. The reflectance spectrum of ARG 2 leached for various periods is shown in Figure 11.

Refractive index, volume fraction and film thickness versus leaching time. From Figure 11 the maximum and minimum reflectivities and the wavelengths at which they occur can be determined for each leaching time. These values may be used in Equations 10 and 11 to determine the refractive indices n_2 and n_2' at the air and glass boundaries of the graded-index layer and the thickness of the layer. Equation 4 may then be used to give the volume fraction of glass remaining at the air side V_a and glass side V_g of the layer. These results are summarized in Table 4 and Figure 12.

Scattering loss in phase separated glass. Because phase-separated glass is inhomogeneous, loss due to Rayleigh scattering occurs. Figure 13 shows the measured loss for ARG 2. The loss coefficient is proportional to λ^{-4} as predicted by Rayleigh scattering theory.[44]

Table 3. The Properties of ARG 2. From Y. Asahara and T. Izumitani, Reference 43.

	BK 7	BK 3	ARG 2
n_d	1.51680	1.49831	1.49596
T_g (°C)	555	550	495
T_s (°C)	615	605	573
α (10^{-7}/°C)	87	59	54
D_a (wt%loss) ($0.01N.HNO_3$, 100°C, 1h)	0.04	0.13	0.39
D_w (wt%loss) (H_2O, 100°C, 1h)	0.13	0.29	0.21

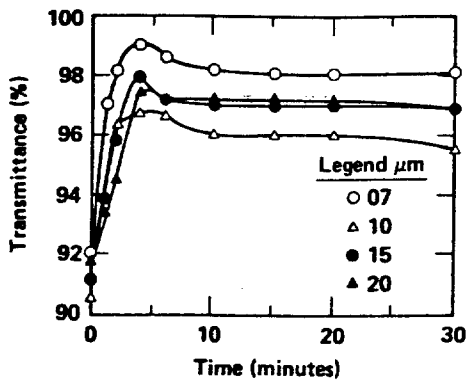

Figure 9: Transmittance of Code 7740 glass as a function of time of treatment in 0.6 wt% NH_4 dissolved in 0.16 HNO_3. From T. H. Elmer and F. W. Martin, Ref. 41.

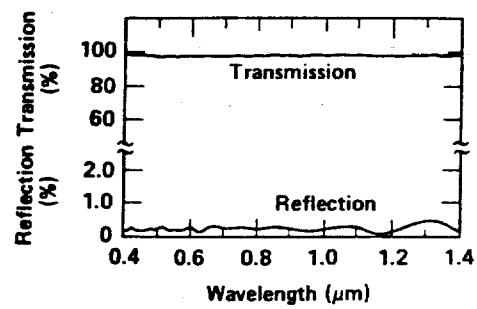

Figure 10: Transmission and reflection of ARG 2 vs. wavelength: The sample was heat treated for 3 hours at 570°C and leached at 75°C for 10 minutes. From Y. Asahara and T. Izumitani, Ref. 43.

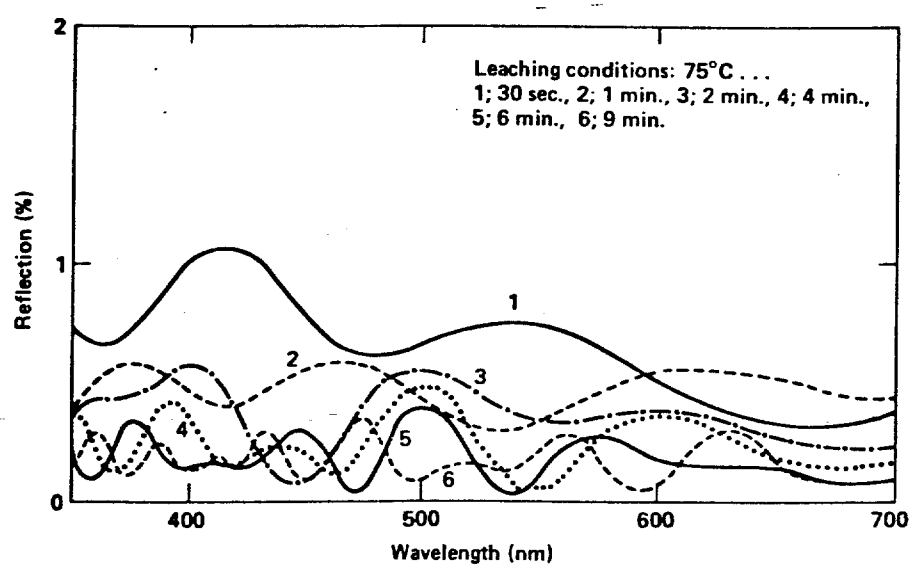

Figure 11: The change in reflection curves of ARG 2 with leaching time. From Y. Asahara and T. Izumitani, Reference 43.

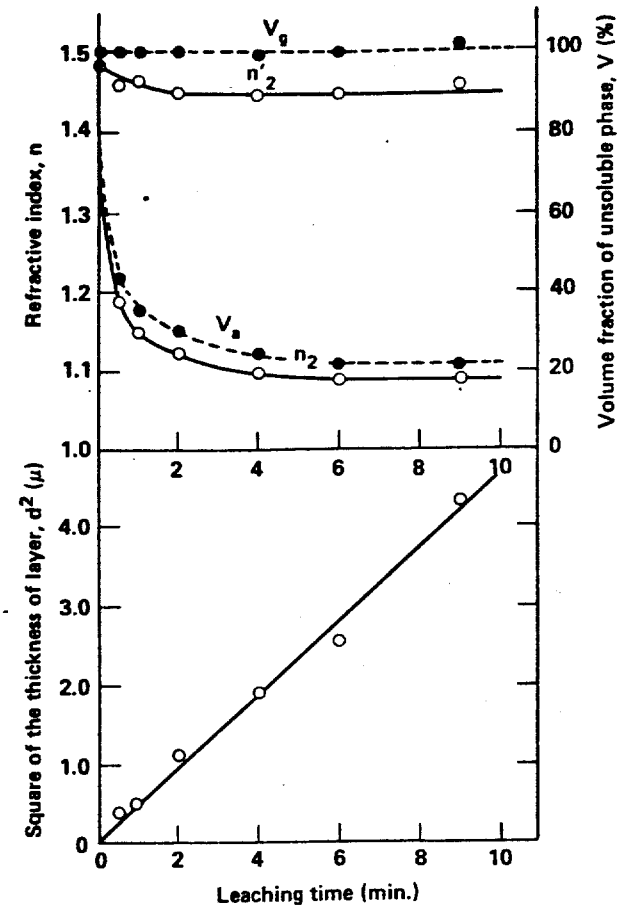

Figure 12: Refractive index, volume fraction and thickness of the antireflection layer versus leaching time. From Y. Asahara and T. Izumitani, Reference 43.

Durability. Data given in Table 4 show that the Knoop hardness of ARG 2 after leaching is about one-third the value of the original glass before leaching. The reduced hardness after leaching is due to the porous structure of the surface. The leached surface can be gently cleaned with lens tissue and solvent without significant change in reflectivity. However, slight scratching can be observed using a microscope.

Neutral Solution Processing

The Neutral Solution Process, developed by Schott Optical Inc.[45,46] produces graded-index surfaces on borosilicate glass, such as BK-7, without the requirement of phase separation. This process is currently used to develop AR surfaces on optical components up to 90 cm diameter for high power Nd-glass lasers.[47]

The Neutral Solution Process derives from studies by Schroeder[48-50] of corrosion of alkali silicate glass by neutral and weakly alkaline solutions of electrolytic salts such as NaCl, LiCl, $NaHAsO_4$ and $NaC_2H_3O_3$. Schroeder proposed that porous, low-index surface layers were formed by the competing processes of partial leaching and total dissolution or etching. The porosity of films formed in "neutral" solutions depends, for a given glass, on the pH and composition of the solution. These and other related studies were reviewed by Schroeder[51] and Kinosita.[52] The process has also been used to prepare AR surfaces on other borosilicates, crown glasses, lead silicate optical and opthalmic glasses and silicate-based laser glasses, demonstrating its wide range of applicability.[46]

Sample preparation. BK-7 glass disks were ground and lapped using 12.5μm diamond grit and polished with CeO_2. Plastic pads were used for grinding and polishing.

Graded-index surface formation. Samples were loaded into polypropylene racks and placed in a solution of 0.03M sodium arsenate and 1.3×10^{-3} M Al^{3+} at 87°C. Solution pH was 7.7.

Table 4. Refractive index, volume fraction and thickness of the gradient-index layer as a function of leaching time. From Y. Asahara and T. Izumitani, Reference 43.

	Leaching Time (min)	Average R_{max}(%)	R_{min}(%)	Refractive Index n_2	n'_2	Volume Fraction V_a(%)	V_g(%)	Thickness d(μ)	Knoop Hardness H_k(kg/mm^2)
1	0	4.05	4.05	1:495	1.495	100	100	0	806
2	0.5	0.908	0.552	1.185	1.465	43	101	0.63	-
3	1.0	0.587	0.370	1.148	1.472	35	102	0.71	-
4	2.0	0.500	0.203	1.123	1.458	30	100	1.07	257
5	4.0	0.368	0.109	1.098	1.455	24	99	1.38	-
6	6.0	0.301	0.089	1.088	1.459	21	100	1.58	-
7	9.0	0.261	0.104	1.087	1.468	21	102	2.13	-
8	20.0	-	-	-	-	-	-	-	123
9	60.0	-	-	-	-	-	-	-	35.6

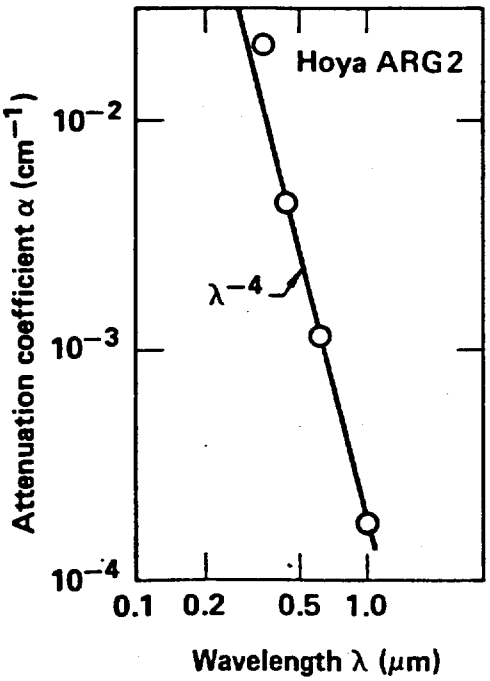

Figure 13: Attenuation coefficient as a function of wavelength for ARG 2 phase-separated glass.

Treatment solutions were contained in polypropylene tanks held in a constant temperature bath.

To stop leaching, samples were soaked in distilled water at 20°C for 2 min, then rinsed in clean spectroscopic grade methanol for 2 min and dried under vacuum of 2.3 kPa for 30 min.

Reflectance versus treatment time. For treatment times of 10-45 hr the reflectance spectrum showed a single broad minimum in the visible or near infrared.

The wavelength of minimum reflectance increased with increasing treatment time as shown by Figure 14.

Reflectance and transmittance data at the reflectance minimum for varying treatment times are given in Table 5.

Reflectance and transmission versus wavelength. The reflectance spectrum shown in Figure 15 was recorded for a sample processed for 39 hours, giving a minimum reflectance at 1.04μm of 0.01%. The transmittance through the sample at 1.04μm was 99.3%.

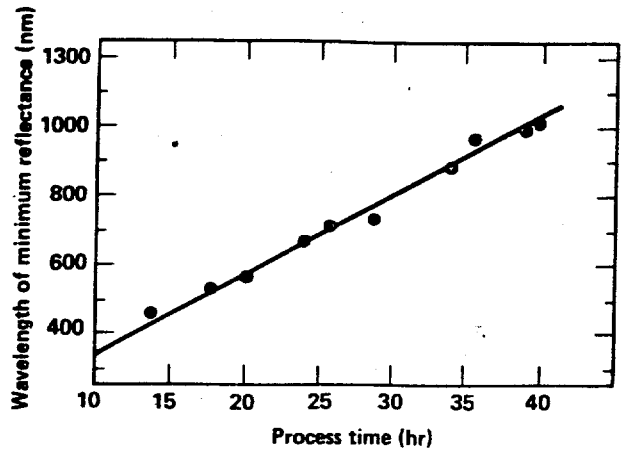

Figure 14: Wavelength of minimum reflectance versus processing time for BK-7 surfaces. From Cook et al, Reference 46.

Figure 16 shows the spectrum of a surface processed for optimum transmission simultaneously at 1.06μm and 0.53μm. These results were achieved in a production facility at Lawrence Livermore National Laboratory which can process surfaces up to 100 cm diameter.[47]

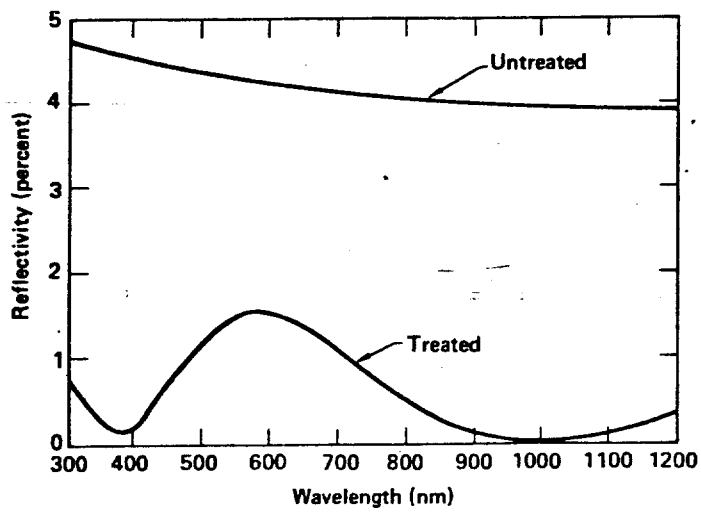

Figure 15: Reflectance spectrum of BK-7 before and after Neutral Solution Processing. From Cook et al, Reference 46.

Influence of surface polishing on film formation. Significant differences in the rate of film formation were observed when different polishing techniques were used. Table 6 gives results for two different treatment times applied to BK-7 polished by various processes.

Light Scattering and Absorption. Marker et al[53] measured loss due to light scattering and absorption as a function of wavelength for BK-7 treated by Neutral Solution Processing. Polished samples of fine-annealed, tank-melted BK-7, 1 cm thick were prepared with reflectance minimum near 1.06μm.

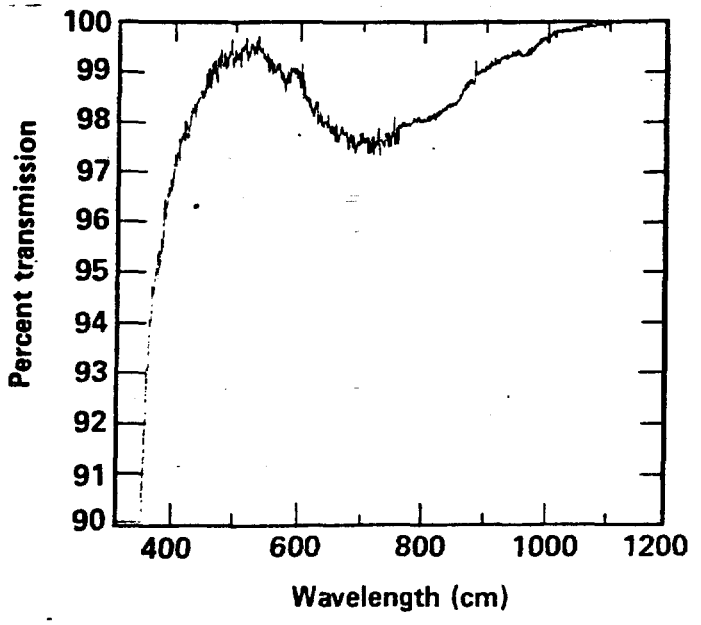

Figure 16: Transmission versus wavelength through 1 cm thick BK-7 processed for optimum transmission simultaneously at 1.06μm and 0.53μm. From Wirtenson et al, Reference 47.

Table 5. Coatings Produced by Neutral Solution Process at 87°C on BK-7 Optical Borosilicate Glass*. From Cook et al, Reference 46.

Sampling time (h)	Wavelength of min. reflectance	%Reflectance at min.	%T at min.
4	no single minimum	8% R 530 nm	91.8% T 530 nm
6	no single minimum	6.8% R 530 nm	93.0% T 530 nm
10	270 nm	0.01%	N.A.
14	448 nm	0.05%	99.5%
17	510 nm	0.05%	99.8%
18	525 nm	0.05%	99.8%
20	555 nm	0.10%	99.7%
24	660 nm	0.10%	99.7%
26	710 nm	0.10%	99.8%
28	738 nm	0.10%	99.7%
34	895 nm, 358 nm	0.30%, 0.25%	99.5%, 92%
36	960 nm, 365 nm	0.20%, 0.3%	99.6%, 91%
38	1000 nm, 390 nm	0.20%, 0.15%	99.0%, 91%
39	1040 nm, 370 nm	0.01%, 0.10%	99.3%
45	1400 nm, 550 nm	0.2%, 0.21%	99.5%, 99.5%

*Reflectance and transmittance data for two surfaces $\theta_i = 10°$

Table 6. Comparison of Polishing Techniques Used in Neutral Solution Process at 87°C on Optical Borosilicate Glass*. From Cook et al, Reference 46.

Polishing Technique	A	B	C	D	E	F
18 hours						
a) wavelength of minimum reflectance	510 nm	N.A.	N.A.	480 nm	480 nm	525 nm
b) % reflectance at minimum	0.15%	N.A.	N.A.	0.07%	0.07%	0.05%
24 hours						
a) wavelength of minimum reflectance	640 nm	850 nm	850 nm	750 nm	750 nm	660 nm
b) % reflectance at minimum	0.10%	0.15%	0.15%	0.15%	0.15%	0.10%

*A = hand polished with plastic pad, B = pitch polished by hand, C = felt polished by hand, B = B etched 1:1 HF/H_2SO_4 5 min at 20°C, E = B etched 48% HF 5 min at 20°C, F = machine polished, plastic pad.

Table 7 summarizes the values of transmission, T, reflectance, R, and loss measured for wavelengths of 0.35-1.06μm. Internal loss due to absorption, A_i, and scattering, S_i, is determined from the exponential loss coefficient $\alpha_i = \ln \frac{T_1/T_2}{D}$ where T_1 and T_2 are the transmission through two samples of differing thickness and D is the difference in thickness in units of cm. The total internal loss is $A_i + S_i = (1-\exp-\alpha_i) = 1 - \frac{T_1/T_2}{D}$ The loss due to surface scattering is $S_s = 1-(A_i+S_i+T+R)$.

Table 7. Values of transmission T, two-surface reflectivity R, internal loss coefficient α_i, internal loss due to absorption A_i and scattering S_i, and surface scattering loss S_s. After Marker et al, Reference 53.

λ(nm)	T(%)	R(%)	$\alpha_i(cm^{-1})$	A_i+S_i	S_s
350	94.8	1.4	2.99×10^{-2}	.029	0.009
400	99.1	0.4	0.241	.002	0.003
450	99.4	0.4	0.281	.003	0.000
500	98.5	1.4	0.200	.002	0.000
550	97.3	2.4	0.120	.001	0.002
600	96.8	3.0	0.160	.002	0.000
650	96.3	3.2	0.200	.002	0.003
700	96.7	2.9	0.120	.001	0.003
750	97.2	2.6	0.080	.001	0.001
800	97.6	2.2	0.080	.001	0.001
1060	99.6	0.3	0.040	0	0.001

Surface figure. Figure 17 shows interferograms taken before and after treatment. No significant change in surface figure was observed.

Variation of reflectivity with angle of incidence. The reflectivity versus angle of incidence for light polarized parallel or perpendicular to the plane of incidence is shown in Figure 18.

Refractive index profile. Using Equations 10 and 11 for the linear-ramp index profile with the values from Figure 15, $R_{min} = 10^{-4}$ at 1.04μm, $R_{max} = 1.5 \times 10^{-2}$ at 0.51μm and $n_g = 1.507$, gives $n_2 = 1.142$, $n'_2 = 1.346$ and d = 0.21μm. The reflectance spectrum calculated using Equation 8 with these values gives nearly exact agreement with the measured spectrum in Figure 15.

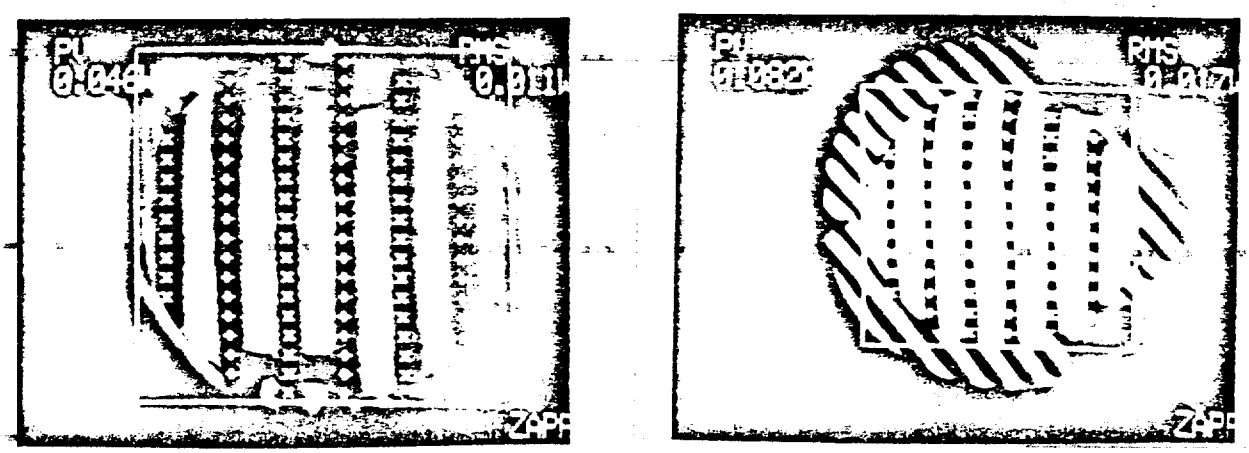

Figure 17: Interferogram of optically flat BK-7 sample 23 cm in diameter before treatment (left) and after treatment (right) to produce minimum reflectivity at 1.06μm. From Cook et al, Reference 46.

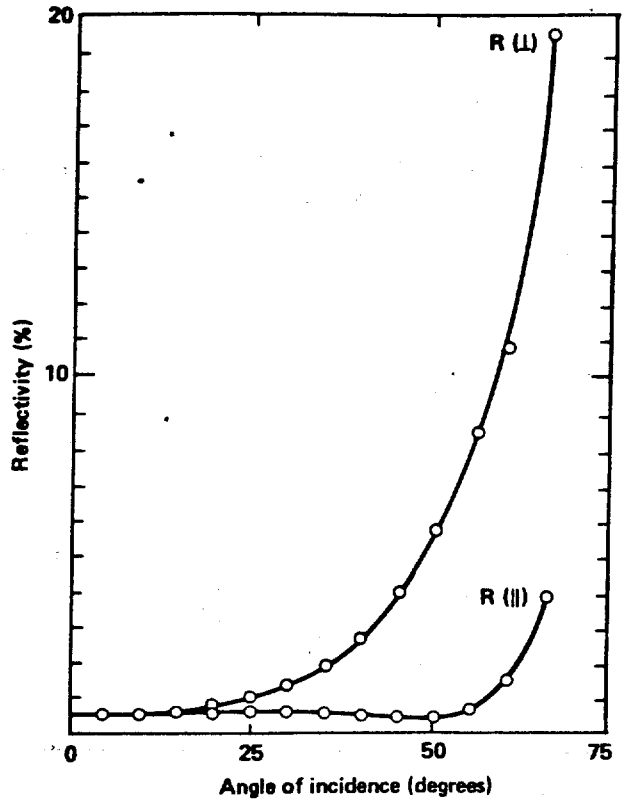

Figure 18: Two-surface reflectivity versus angle of incidence for light polarized parallel ($R_{||}$) and perpendicular ($R_{\perp}$) to plane of incidence for BK-7 surface after Neutral Solution Process for 28 hours. From L. M. Cook, unpublished.

Durability. Surfaces are sufficiently durable to be cleaned with lens tissue and alcohol without visible change of reflectance. However, inspection with a stereomicroscope at 100X magnification revealed minor scratches.

No measurable change in reflectivity was observed after aging two months at 50% relative humidity.

Graded-index Coatings

Techniques reviewed in the preceding sections can produce graded-index surfaces only on materials with appropriate leachable components. Graded-index coatings which can be applied to a wide variety of substrate materials greatly increase the range of applications. Coatings of non-crystalline, multicomponent, inorganic, oxide films can be deposited by the sol-gel process and subsequently etched, with or without phase separation, to produce graded-index AR surfaces.

The sol-gel process consists of polymerization of a viscous liquid sol of alkoxysilane with other metal alkoxides or metal salts in alcoholic solutions to form a transparent elastic gel. The residual organic material is removed by heating, leaving a microporous structure. The pores can often be eliminated by further heating, without melting, to form a glass-like material.

The term "sol-gel" has come to be applied to a variety of processes by which dielectric films are deposited from solutions. Geffcken and Berger[54] initially prepared films of SiO_2. Their work was later extended by Geffcken[55] to other oxides of Group IV elements. Interest in such films declined due to advances in vacuum coating methods, which were more economical for small parts. Further development was stimulated by requirements for optical coatings over large surface areas. Schroeder[56] found that oxide layers could be obtained

with elements of most groups of the periodic table. Properties and applications of a wide variety of single and mixed oxide films are reviewed by Schroeder[57] and by Dislich and Hussmann.[58] Recently, Yoldas[59] used the porous nature of the initial film before densification to create a single-layer AR film of Al_2O_3 on soda-lime glass. Films of multicomponent oxide glass were developed by Dislich and Hinz[60-62] and by Levene and Thomas.[63]

McCollister and Boling[64] used the sol-gel process to deposit a multicomponent glass film of a composition that could phase separate. Then, the film was heated to cause phase separation and one phase was preferentially removed by leaching and etching to form a porous, graded-index layer. One possible coating solution, and the results achieved in coating fused silica are as follows:[64]

Coating solution. Tetraethyl silicate (24.5 g) was mixed with methoxyethanol (25 g) and 1 N nitric acid solution (2.4 g) was added. The resulting solution was heated to approximately 60°C and then allowed to cool to room temperature. Aluminum tri-sec-butoxide (3.1 g) was added and the mixture stirred until a clear solution was obtained. Calcium nitrate tetrahydrate (4.6 g), sodium nitrate (1.1 g) and magnesium basic carbonate (1.8 g) were dissolved in water (20 g) and concentrated nitric acid (10 g). The solution was then added to the aluminosilicate solution and the resulting solution made up to a total weight of 200 g with isopropanol. The product contained the equivalent of 10 g total oxides in 200 g total.

The composition of the solution was such that, when heated to drive off volatiles and decompose the organic portions, the resulting glass has the composition given in Table 8.

Table 8. Composition of graded-index sol-gel coatings applied to fused silica.

Component	Parts by Weight Coating 1*	Coating 2†
SiO_2	70	84
Al_2O_3	6.4	--
CaO	10.9	--
MgO	7.8	--
Na_2O	3.9	4
B_2O_3	--	12

* From H. L. McCollister and N. L. Boling, Reference 64.
† From S. P. Mukherjee and W. H. Lowdermilk, Reference 66.

Deposition. One fourth of a 2.5 inch disk, 1.7 mm thick of polished, fused silica was spin coated on a turntable with 6 drops of the solution. The spinning spread an even coat of the solution over the surface. After the coating was dry to the touch, the second side was coated in the same manner. The coated sample was then dried for 15 min at 85°C.

Heat treatment. The coating was consolidated by heating for 20 min at 300°C. Phase separation was then effected by heating for one hour at 750°C.

Etching. Both sides of the sample were etched by immersing for two minutes in a solution containing 1.2 ml of a 47 wt% solution of HF in water, 7.6 ml of a 37 wt% of HCl in water and 112 ml of alcohol consisting of 90.2 wt% ethanol, 4.8 wt% methanol, and 5 wt% isopropanol. Then the sample was rinsed in water with ultrasonic agitation. The etched and leached sample was then air dried under a heat lamp, leaving a porous coating on each side. The etched and leached portion was about 0.25μm thick and the porosity was highest at the surface, gradually decreasing away from the surface. The pore size of the voids nearest the surface was about 100-200 Å across.

Transmission of coated sample. The transmission of the silica and of the sample containing the phase separated, etched and leached coating for various wavelengths was run on a Cary 14 spectrophotometer. Results are given in Table 9. McCollister and Boling[64] give examples of additional coating solutions and substrates.

Table 9. Transmission of fused silica samples uncoated and coated with phase-separated, etched and leached coating for various wavelengths. From H. L. McCollister and N. L. Boling, Reference 64.

Wavelength nm	Transmission Uncoated	Coated
400	92	96.5
500	--	97
600	--	99.9
700	93.2	99.5
800	--	99
900	--	98.2
1000	--	97.8
1100	--	96.8
1200	94	--
1500	94	96
2000	93.5	95

Independently, Mukherjee[12,65,66] developed a single-layer, gradient-index AR coating based on the following steps: (1) prepare a partially polymerized solution from metal alkoxides; (2) develop multicomponent non-crystalline glass-like transparent gel-derived coatings with a leachable phase and/or porous microstructure; (3) leach the leachable phase and/or change the pore morphology in a controlled way so that a refractive index gradient develops. A description of that process and results are as follows:

Coating solution. The coating solution was prepared by mixing tetramethoxysilane with twice its volume of anhydrous ethanol at room temperature. The solution was heated to 40°C. A controlled amount of water [0.33 mol per mol of $Si(OCH_3)_4$] acidified with dilute HCl was added for partial hydrolysis of $Si(OCH_3)_4$. Small amounts (5-7 vol%) acetylacetone was added and the solution was stirred at 40°C for 1 hour. The pH of the solution at this stage was 4-5. Then, boric acid dissolved in hot anhydrous methanol was added and the solution was stirred for 3 hours. Finally, sodium methylate dissolved in anhydrous methanol was added. The solution was stirred for 15 min at 40°. The solution was further diluted with anhydrous ethanol to 0.04 g/ml metal oxide before deposition of the coatings. This solution gave coatings with the glass composition given in Table 8.

Substrate preparation. Test films were applied to Corning Code 7740, BK-7 glass and fused silica. The substrates were cleaned by a mild etch for 10 min in a 1 wt% NaOH solution at 95°C followed by 2 min in 1 N HCl at 50°C. The substrates were then rinsed with isopropanol and dried overnight at 150°C.

Deposition. Films were deposited by dipping the substrates in the dilute polymeric solution. Substrates were suspended on a wire, totally immersed in the solution, and then withdrawn vertically at a rate of 5 cm/min using a variable speed motor. Transparent gel films formed on the substrate when the solution was exposed to atmospheric moisture.

Thickness of the coatings was built up by multiple dipping. After each dipping, the deposited layer was allowed to dry in air for a minimum of 15 min. Substrates have been coated with ten layers without losing transparency. No systematic study was made of the thickness of each layer or the densification of films at different temperatures. However, the thickness of two multilayer films measured after drying at 150°C indicated that each dipping added a thickness of 325 Å.

Heat treatment. The coated substrates were dried overnight in air under an infrared lamp at 80°C. They were then heated in a furnace, with temperature increasing at the rate of 3°C/min, to various heat-treatment temperatures of 350-500°C.

Etching. After heat treatment, samples were leached in a 0.5 wt% hydrofluoric acid solution or a solution of 0.6 wt% sodium fluoride in 0.16N nitric acid for various times between 15 sec and 10 min.

Reflectance of coated sample. Reflectance at 1.06μm wavelength of films with various heat treatments and leaching conditions was measured using a Nd:YAG laser. The results are summarized in Table 10. The reflectance values given in the table are the minimum values observed for each surface. Substantial variation over the surface was observed, with reflectance maxima typically of 2%.

Table 10. Reflectance of sol-gel films at 1.06μm after leaching with 0.6 wt% NH_4F in 16 N HNO_3 at 90°C. From S. P. Mukherjee and W. H. Lowdermilk, Reference 66.

Heat treatment		Leaching time(s)	Reflectance (%)
Temp. (°C)	Time (h)		
350	1.5	15	0.27
350	5.5	15	0.33
500	1.5	15	0.67
500	5.5	15	0.20
350	1.5	30	0.33
350	5.5	30	0.13
500	1.5	30	0.23
500	5.5	30	0.13

Graded-index Surfaces Produced by Ion Implantation

Spiller et al[67] reported producing a graded-index layer on plastic surfaces by bombarding them with high energy ions and subsequently etching the particle tracks. The high energy particles produce damage tracks when passing through the solid. A properly chosen etchant can widen those tracks to produce a microporous surface.

The shape of the etched track is determined by the ratio of etch rates in the damaged and undamaged areas. To form an effective AR layer, the etched tracks must form narrow cones with a depth > $\lambda/2$ and the spacing between tracks must be << λ to prevent large scattering losses. The process and results are summarized below.

Samples treated. Biphenol-A polycarbonate plates 3.2 mm thick (General Electric Co., Lexan) Polyethylene terephthalate sheets 0.076 mm thick (E. I. Dupont, Mylar D).

Irradiation. Samples were irradiated on one or both sides with ions from a 2 MeV Van de Graaff generator. Results were reported for irradiation by helium and carbon ions.

Etch procedure. Samples were immersed in 6N sodium hydroxide solution typically for 4 min at 60°C, rinsed in deionized water and dried.

Surface reflectivity. Reflectivity and increase in transmission of the polycarbonate window are shown in Figure 19. Results obtained on the Mylar films are shown in Figure 20. The curves in Figure 20 show the difficulty of obtaining low reflectivity in the IR and, simultaneously, low scattering loss in the UV. Low scattering in the UV can be obtained only with very dense, fine tracks which are produced by a short etching time. To obtain low IR reflectivity, the etch time must be increased to make the depth of the etch pits > $\lambda/2$ for IR wavelengths. However, with long etch time, the pits widen and structure becomes coarser which increases UV scattering.

In principle, this technique is widely applicable because damage track formation has been observed in a large number of materials.[68] Parameters which determine whether an effective graded-index AR surface can be formed are:

a. The energy loss rate of the particle within the material, which affects the differential etch rate.[69]
b. The exposure dose, which determines the average spacing between tracks.
c. The selection of etchant and etching time.

Stephens and Cody[3] bombarded fused silica with 63 MeV copper ions to a density of about $10^{12}/cm^2$ and etched for a few minutes in 2.5 wt% ammonium hexafluoride solution. The resulting surfaces had reflectivity of ∿ 2% in the visible with substantial scattering loss in the UV.

Recent experiments by Hopper[70] have shown the possibility of forming AR surfaces on various optical glasses by bombarding the surfaces with uranium fission fragments and etching the damage tracks. Tests also have been conducted on fused silica. However, only low differential etch rates have been achieved which produce wide, shallow cones leading to large scattering losses in the UV.

"Moth's Eye" Antireflection Surfaces

Graded-index AR surfaces occur in nature. Bernhard[71] discovered that the cornea of nocturnal insects is covered by arrays of fine protuberances, which he called corneal nipples. He proposed that the purpose of these arrays was to reduce reflectance of the

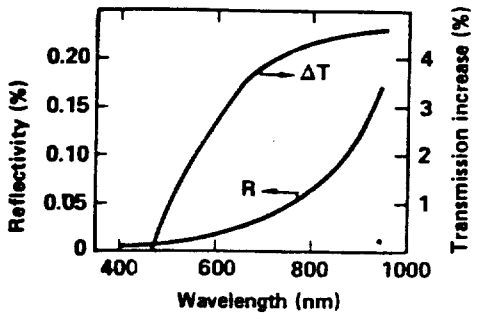

Figure 19: Measured reflectivity R of a polycarbonate window and increase in transmission ΔT. R and ΔT are normalized to one surface; the decrease in transmission for blue light is due to scattering. From E. Spiller et al, Reference 67.

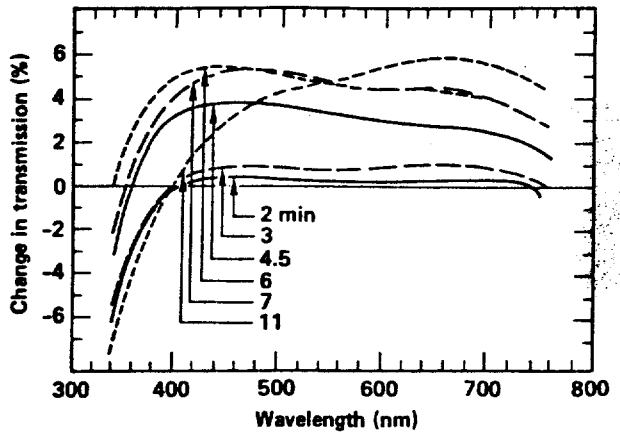

Figure 20: Change of the transmission vs wavelength of a foil of Mylar D (thickness = 80μ) exposed on one side to a flux of $\sim 10^{12} cm^{-2}$ carbon ions with 2-MeV energy and developed in 6N NaOH at temperature of 35°C with the development time as a parameter. Heavy exposure produces a decrease in transmission of wavelengths $\lambda < 400$ nm, which can be recognized by some yellow coloration of the sample even before development. Increasing development time reduces the reflectivity and increases the transmission. At $\lambda = 400$ nm maximum transmission is obtained for a development time of 6 min. Longer development results in increased scattering, which decreases the transmission again. From E. Spiller et al, Reference 67.

surface of the eye and thereby improve the insect's camouflage. The nipples had both height and spacing of about 2000 Å which provide a graded transition of refractive index between the air and the cornea. Bernhard's proposal was substantiated by measurements with microwave radiation reflected from a model of the array, scaled up appropriately for the longer wavelengths.

Similar surfaces to those of the moth's eye were prepared in photoresist by Clapham and Hutley.[72] They recorded straight line interference fringe patterns from two krypton laser (351 nm) beams intersecting at 120°, giving a fringe spacing of 210 nm. The array structure was formed by superimposing two such patterns at right angles. Scanning electron micrographs of the natural and photofabricated surfaces as well as the reflectance spectrum are given by Hutley.[73] The integrated white light reflectance was reduced from 5.5% to 0.35%, which compares well with commercial multilayer coatings.

Optimization of a moth's eye and other corrugated surfaces for minimum reflectance has been discussed by Thornton.[74] He concluded that a 30dB reduction in reflectance could be achieved over a bandwidth of 1.4 times the short wavelength limit of the band.

Laser-induced damage to graded-index AR surfaces

An important stimulus to recent developments in graded-index AR surfaces was the discovery by Lowdermilk and Milam[8,9] that the surfaces had significantly higher threshold for laser-induced damage than conventional, vacuum-deposited AR coatings. A comparison of damage thresholds of graded-index surfaces and SiO_2/TiO_2 thin-film AR coatings is given in Figure 21. These thresholds were measured with 1 ns, 1.06μm pulses from a Nd-glass laser. The graded-index surfaces were formed by leaching phase-separated glass. Damage thresholds of graded-index surfaces formed on non phase-separated glass are shown in Figure 22. The threshold of these surfaces may be further increased by irradiating them with laser pulses at fluence levels below the initial damage threshold.[11] Damage thresholds of graded-index coatings deposited by the sol-gel process are shown in Figure 23.

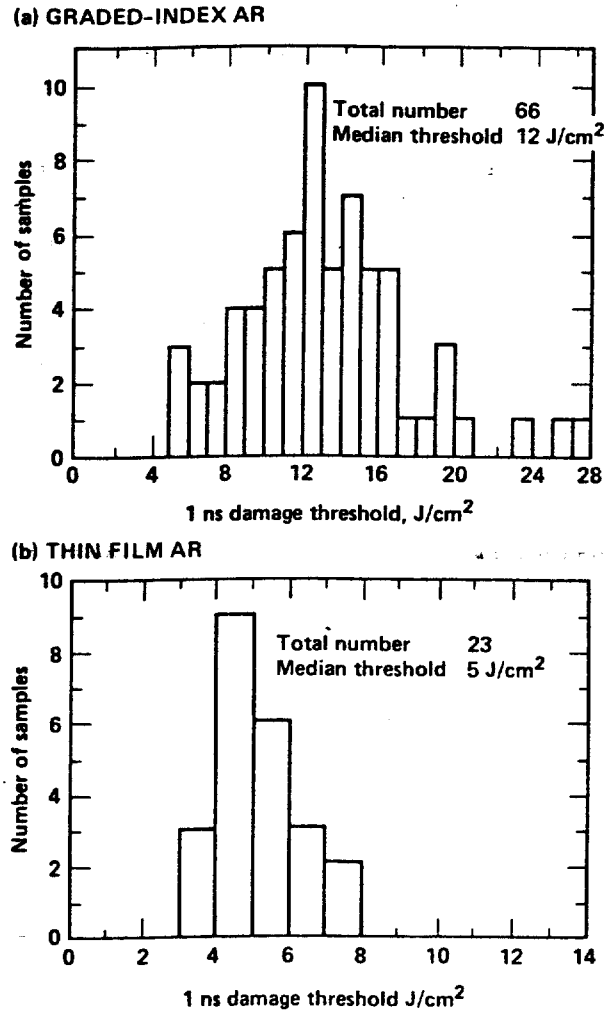

Figure 21: Histogram of 1 ns, 1.06μm laser-pulse damage thresholds of (a) graded-index AR surfaces on phase-separated, leached and etched glass, (b) SiO_2/TiO_2 thin-film AR coatings. From W. H. Lowdermilk and D. Milam, Reference 8.

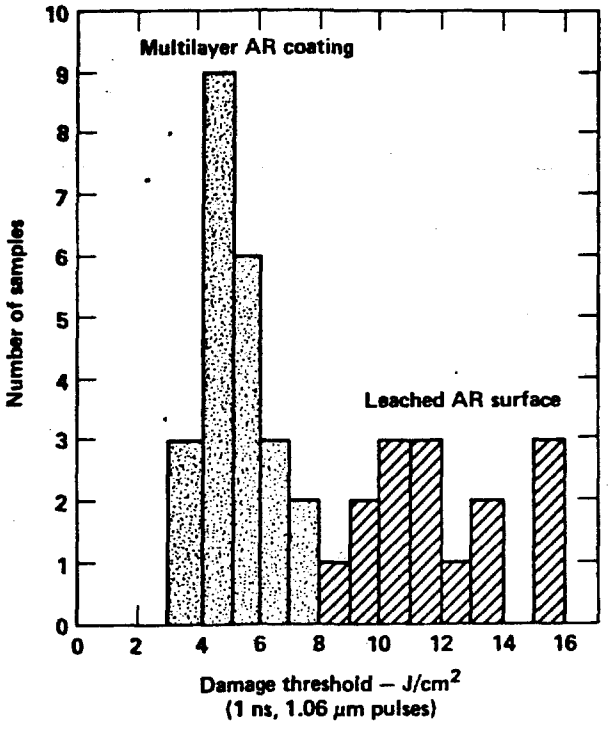

Figure 22: Histogram of laser damage thresholds for leached AR surfaces on BK-7 produced by the Neutral Solution Process and for SiO_2/TiO_2 thin-film AR coatings. Thresholds were measured with 1 ns, 1.06 μm laser pulses. From L. M. Cook et al, Reference 10.

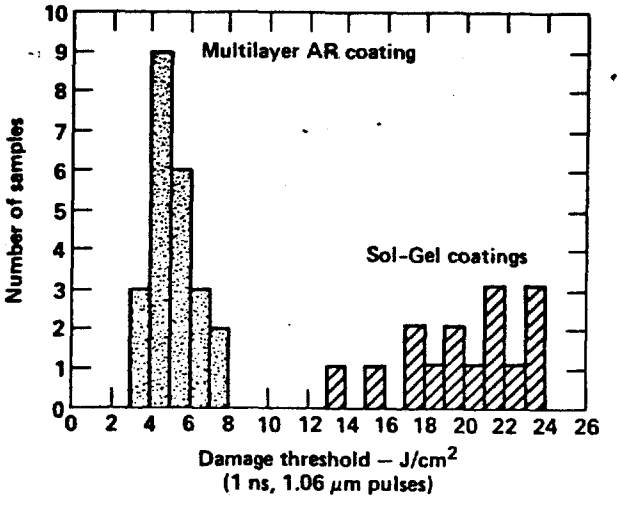

Figure 23: Histogram of laser damage thresholds for sol-gel AR coatings and SiO_2/TiO_2 thin-film AR coatings. Thesholds were measured with 1 ns, 1.06μm laser pulses. From S. P. Mukherjee and W. H. Lowdermilk, Reference 12.

Damage to vacuum deposited AR coatings has been studied extensively.[75] Coating damage results from absorption of energy. If absorbing particles are trapped at the glass-coating interface, exposure to high energy laser pulses causes them to vaporize, thus damaging the coating.

The high damage threshold of graded-index surfaces is thought to be a consequence of the integral nature of the surface. First, interface inclusions do not occur since there is no interface, and, in addition, the leaching process may remove particulate impurities.

Second, bond strength between the graded-index surface layer and the glass is that of the glass itself, which reduces the possibility for delamination. Finally, the surface layer should have low internal stress because the leaching process preferentially attacks stressed bonds.

Conclusion

Graded-index surfaces have had a long and interesting history; beginning over a century ago as a scientific curiosity. Techniques for producing graded-index AR surfaces finally reached commercial application only to be almost immediately replaced by vacuum-deposited coatings. After laying dormant for forty years, interest in graded-index surfaces was revived by important applications in solar collectors and high power lasers. These and other applications such as optical disk and various anti-glare surfaces are stimulating new developments in materials and techniques for providing graded-index surfaces and films.

References

1. Meinel, A. B., and Meinel, M. P., Applied Solar Energy, Addison Wesley, Reading, MA, 1976, Sections 9.13-9.17.
2. Stephens, R. B., and Cody, G. D., Optical reflectance and transmission of a textured surface, Thin Solid Films, 45, 19, 1977.
3. Stephens, R. B., and Cody, G. D., Inhomogeneous surfaces as selective solar absorbers, Solar Energy Materials 1, 397, 1979.
4. Cuomo, J. J., Ziegler, J. F., and Woodall, J. M., A new concept for solar energy thermal conversion, Appl. Phys. Lett. 26, 557, 1975.
5. DiStefano, T. H., Pettit, G. D., Woodall, J. M., and Cuomo, J. J., Conformal antireflective coatings on textured tungsten surface, Appl. Phys. Lett. 32, 676, 1978.
6. Haggerty, J. S., Graded index antireflective coatings for glass, Final Report to the Dept. of Energy, Agreement No. DE-AC02-78ER05003, April 1982.
7. Ritchie, I. T., and Window, B., Applications of thin graded-index films to solar absorbers, Appl. Opt. 16, 1438, 1977.
8. Lowdermilk, W. H., and Milam, D., Graded-index antireflection surfaces for high power laser applications, Appl. Phys. Lett. 36, 891, 1980.
9. Lowdermilk, W. H., and Milam, D., Graded-index surfaces to limit reflection, Laser Focus 16, 64, 1980.
10. Cook, L. M., Lowdermilk, W. H., Milam, D., and Swain, J. E., Antireflective surfaces for high energy laser optics formed by neutral solution processing, Appl. Opt. 21, 1482, 1982.
11. Swain, J. E., Lowdermilk, W. H., and Milam, D., Raising damage thresholds of gradient-index antireflecting surfaces by pulsed laser irradiation, Appl. Phys. Lett. 41, 782, 1982.
12. Mukherjee, S. P., and Lowdermilk, W. H., Gradient-index AR film deposited by the sol-gel process, Appl. Opt. 21, 293, 1982.
13. Jacobsson, R., Light reflection from films of continuously varying refractive index, in Progress in Optics, Vol. 5, Wolf, E., Ed., North Holland Publishing Co., Amsterdam, 1978, chap. 5.
14. Monaco, S. F., Reflectance of an inhomogeneous thin film, J. Opt. Soc. Am. 51, 280, 1961.
15. Knittl, Z., Optics of Thin Films, John Wiley and Sons, London, 1976, pp. 429-79.
16. Born, M., and Wolf, E., Principles of Optics, Pergamon Press, London, 1970 (Fourth Edition), p. 58.
17. Sheldon, B., Haggerty, J. S., and Emslie, A. G., Exact computation of the reflectance of a surface layer of arbitrary refractive index profile and an approximate solution of the inverse problem, J. Opt. Soc. Am. 72, 1049, 1982.
18. Schroeder, H., Remarks on the theory of light transmission through inhomogeneous transparent layers (in German), Ann. Phys. 39, 55, 1941.
19. Minot, M. J., The angular reflectance of single-layer gradient refractive-index films, J. Opt. Soc. Am. 67, 1046, 1977.
20. Fraunhofer, J., Experiments on the cause of tarnishing and fogging of glasses and methods to avoid them, 1817 (in German), in Gesammelte Schriften, Lommel, E., Ed., Munchen, 1888, pp. 35, 46.
21. Lord Rayleigh, On the intensity of light reflected from certain surfaces at nearly perpendicular incidence, Proc. R. Soc. London 41, 1886, 275.
22. Cook, L. M., and Mader, K.-H., Integral antireflective surfaces on optical glass, Opt. Eng. 21, SR-010, 1982.
23. Taylor, H. D., On the adjustment and testing of telescopic objectives 1891, reprinted by Grubb, Parsons & Co., 1946, p. 62; British Patent 29561.
24. Kollmorgen, F., Light transmission through telescopes, Trans. Illum. Eng. Soc. 11, 22, 1916.
25. Amy, M. P., Contribution to the study of glass reflection, Rev. Opt. 6, 305, 1927.

26. Jones, F. L., and Homer, H. L., Chemical methods for increasing the transparency of glass surfaces, J. Opt. Soc. Am. 31, 34, 1941.
27. Nicoll, F. H., New chemical method of reducing reflections of glass, RCA Review 6, 298, 1942.
28. Nicoll, F. H., and Williams, F. E., Properties of low reflection films produced by the action of hydrofluoric acid vapor, J. Opt. Soc. Am. 33, 434, 1943.
29. Nicoll, F. H., and Williams, F. E., A method for producing low-glare coatings, U. S. Patent 2, 486, 431, 1949.
30. Thomsen, S. M., Skeletonizing glass, U. S. Patent 2, 490, 662, 1949.
31. Thomsen, S. M., Low reflection films produced on glass in liquid fluorosilic acid bath, RCA Review 12, 143, 1951.
32. Nicoll, F. H., Anomalous interference films on glass by chemical treatment, J. Opt. Soc. Am. 42, 241, 1952.
33. Nicoll, F. H., Low-reflecting glass, U. S. Patent 2, 707, 899, 1955.
34. Holland, L., The properties of glass surfaces, Chapman and Hall, London, 1966, pp. 155, 165.
35. Minot, M. J., Single-layer, gradient refractive index antireflection films effective from 0.35 to 2.5μ, J. Opt. Soc. Am. 66, 515, 1976.
36. Minot, M. J., and Ortabasi, U., Antireflective layers on phase separated glasses, U. S. Patent 4,086,074, April 25, 1978.
37. Doddato, J. A., and Minot, M. J., Durable substrates having porous antireflection coatings, U. S. Patent 4,080,188, March 21, 1978.
38. Vogel, W., Structure and crystallization of glasses (Pergammon, New York, 1971), pp. 60-80.
39. Elmer, T. H., Nordberg, M. E., Carrier, G. B., and Korda, E. J., Phase separation in borosilicate glasses as seen by electron microscopy, J. Am. Ceram. Soc. 53, 171, 1970.
40. Haller, W., Blackburn, D. H., Wagstaff, F. E., and Charles, F. J., Metastable immiscibility surface in the system Na_2O-B_2O_3-SiO_2, J. Am. Ceram. Soc. 53, 34, 1970.
41. Elmer, T. H., and Martin, F. W., Antireflection films on alkali-borosilicate glasses produced by chemical treatments, Ceramic Bulletin 58, 1092, 1979.
42. Power, J. M., and Elmer, T. H., Weathering of graded-index antireflection films on a borosilicate glass, Am. Ceram. Soc. Bull. 59, 1124, 1980.
43. Asahara, Y., and Izumitani, T., The properties of gradient index antireflection layer on the phase separable glass, J. Non-Crys. Solids 42, 269, 1980.
44. Kerker, M., The scattering of light, Academic Press, New York, 1969, p. 33.
45. Cook, L. M., Mader, K.-H., and Schnabel, R., Integral antireflective surfaces on silicate glass, U. S. Pat. Appl. 309, 149, Oct. 6, 1981.
46. Cook, L. M., Ciolek, S., and Mader, K.-H., Integral antireflective surface production on optical glass, J. Am. Ceram. Soc. 65, C152, 1982.
47. Wirtenson, G. R., Brown, N. J., and Cook, L. M., Scaling up the neutral solution anti-reflection process, in Laser Induced Damage in Optical Materials: 1982, Bennett, H. E., Guenther, A. H., Milam, D., and Newnam, B. E., Eds., in press.
48. Schroeder, H., On the corrosion of glass by solutions with pH value near 7 (in German), Glastech. Ber. 26, 91, 1953.
49. Schroeder, H., Method to increase the transmission and reduce the reflectivity of glass or similar materials (in German), West German Patent 821828, 1952.
50. Schroeder, H., A method of reducing surface reflectivity from articles of glass or silicates, British Patent 698,831, 1953.
51. Schroeder, H., Thin film formation on glass surfaces in chemical coating processes, The Tenth International Congress on Glass, Part 1, Kunugi, M., Tasahiro, M., Soga, N., Eds., The Ceramic Society of Japan 8, 118, 1974.
52. Kinosita, K., Surface deterioration of optical glasses, in Progress in Optics, Vol. 4., Wolf, E., Ed., North Holland Publ. Co., Amsterdam, 1965, chap. 3.
53. Marker, A. J. III, Cook, L. M., and Mader, K.-H., Light scattering in leached antireflection surfaces, SPIE Proceedings Vol. 362 (in press).
54. Geffcken, W., and Berger, E., Method of producing layers on solid objects, Dtsch. Reichspatent 736,411, 1939, (U. S. Pat. 2,366,516, Jan. 2, 1945) Jenaer Glaswerk Schott and Gen., Jena, GDR.
55. Geffcken, W., Thin layers on glass (in German), Glastech. Ber. 24, 143, 1951.
56. Schroeder, H., Properties and applications of oxide layers deposited on glass from organic solutions, Opt. Acta. 9, 249, 1962.
57. Schroeder, H., Oxide layers deposited from organic solutions, in Physics of Thin Films, Vol. 5, Hass, G. and Thun, R. E., Eds., Academic Press, New York, 1969, 87.
58. Dislich, H., and Hussmann, E., Amorphous and crystalline dip coatings obtained from organometallic solutions: procedures, chemical processes and products, Thin Solid Films 77, 129, 1981.
59. Yoldas, B. E., Investigations of porous oxides as an antireflective coating, Appl. Opt., 19, 1425, 1980.

60. Dislich, H., Hinz, P., and Kaufman, R., Preparation of transparent, vitreous, crystalline inorganic multiple component materials, especially in thin layers, at temperatures far below their melting points, F.R.G. Patent 1941, 191, Jan. 14, 1971, Jenaer Glaswerk Schott und Gen., Mainz, F.R.G.
61. Dislich, H., New routes to multicomponent oxide glasses, Angew. Chem. Int. Ed. Engl. 10, 363, 1971.
62. Dislich, H., and Hinz, P., History and principles of the sol-gel process and some new multicomponent oxide coatings, J. Non-Crys. Solids 48, 11, 1982.
63. Levene, L., and Thomas, I. M., Process of converting metal organic compounds and high purity products obtained therefrom, U. S. Pat. 3640093, February 8, 1972, Owens-Illinois, Inc., USA.
64. McCollister, H. L., and Boling, N. M., Process of making glass articles having antireflective coatings and product, U. S. Patent 4,273,826, 1981, Owens-Illinois, Inc., U.S.A.
65. Mukherjee, S. P., Gel-derived single-layer antireflection films with refractive index gradient, Thin Solid Films 81, L89, 1981.
66. Mukherjee, S. P., and Lowdermilk, W. H., Gel-derived single-layer antireflection films, J. Non-Crys. Solids 48, 177, 1982.
67. Spiller, E., Haller, I., Feder, R., Baglin, J. E. E., and Hammer, W. N., Graded index surfaces produced by ion implanation on plastic materials, Appl. Opt. 19, 3022, 1980.
68. Fleischer, R. L., Price, P. B., and Walker, R. M., Nuclear Tracks in Solids, U. California Press, Berkeley, 1975.
69. Enge, W., Grabisch, K., Dallmeyer, L., Bartholoma, K. P., and Beaujean, R., Etching behavior of the Lexan polycarbonate plastic detector, Nucl. Instrum. Methods 127,125, 1975.
70. Hopper, R. W., Lawrence Livermore National Laboratory, Nov., 1982, unpublished.
71. Bernhard, C. G., Structural and functional adaptation in a visual system, Endeavor 26, 79, 1967.
72. Clapham, P. B., and Hutley, M. C., Reduction of lens reflection by the "Moth Eye" principle, Nature 244, 281, 1973.
73. Hutley, M. C., Coherent photofabrication, Opt. Eng. 15, 190, 1976.
74. Thornton, B. S., Limit of the moth's eye principle and other impedance matching corrugations for solar absorber design, J. Opt. Soc. Am. 65, 257, 1975.
75. Lowdermilk, W. H., and Milam, D., Laser-induced surface and coating damage, IEEE J. Quant. Electr. QE-17, 1888, 1981.